Kinetics of signaling-DNA-aptamer–ATP binding

Issei Nakamura* and An-Chang Shi†
Department of Physics and Astronomy, McMaster University, 1280 Main Street West, Hamilton, Ontario, Canada L8S 4L8

Razvan Nutiu,‡ Jasmine M. Y. Yu, and Yingfu Li
Department of Biochemistry and Biomedical Sciences, McMaster University, 1280 Main Street West, Hamilton, Ontario, Canada L8S 4L8

(Received 17 July 2008; revised manuscript received 16 January 2009; published 16 March 2009)

DNA aptamers are molecular biosensors consisting of single functionalized DNA molecules, which can bind to specific targets or complementary DNA sequences. The binding kinetics of DNA aptamers is studied by fluorescence quenching at 23 °C. A kinetic model for the binding reaction of DNA aptamer, antisense DNA, and ATP target is developed to describe experimental observations. The approach leads to a simple procedure to deduce relevant kinetic reactions and their rate constants. A comparison between theory and experiments indicates that the previously established bimolecular DNA-ATP binding does not provide a complete description of the experimental data. Side reactions such as trimolecular complexation are proposed. Rate constants of the model are determined by comparing the model predictions and experiments. Good agreements between the model and experiments have been obtained. Possible blocking reactions by the misfolded DNA aptamer are also discussed.

DOI: 10.1103/PhysRevE.79.031906 PACS number(s): 87.15.R−, 82.39.−k, 87.14.gk

I. INTRODUCTION

Recent development in biochemical engineering allows us to obtain single-stranded nucleic acids capable of ligand binding, referred to as DNA/RNA aptamers. In addition to understanding the binding mechanism of nucleic acids, a large number of potential applications of these molecules as biosensors are expected in proteomics or drug delivery [1]. Several experimental methods have been used to examine the interaction of the aptamers with other biomolecules. For example, the protein-DNA/RNA association is often studied using the electrophoretic mobility shift assay (EMSA) [2–4] or the in-line probing assay which relies on the spontaneous cleavage of RNA depending on secondary and tertiary structures [5,6]. Furthermore, surface plasmon resonance (SPR) is considered as a powerful technique [7] for the study of biomolecular kinetics [8,9]. Although these approaches are useful for analyzing binding reaction of aptamers, they offer limited information for the kinetics or tend to be time consuming and labor intensive. In order to overcome these difficulties, an alternative and more efficient method using a signaling aptamer labeled with a fluorophore, which is created by *in vitro* selection, has been developed [10,11]. In this case, the aptamer undergoes a fluorescence change upon target binding in accordance with the principle of fluorescence resonance energy transfer (FRET) [12]. Since FRET gives rise to a signaling fluorescence intensity in accordance with whether or not the attached fluorophore is in close proximity of the quencher, the method is frequently employed to study the dynamics of nucleic acids such as conformational dynamics of a DNA hairpin loop [13] and DNA breathing [14].

In general, however, target binding may cause alteration of the fluorophore and eventually lead to the failure of the assay. Thus, a stable and reliable aptamer biosensor remains highly desirable [15]. One successful strategy is to covalently modify the aptamer with extrinsic fluorophores. It has been shown that the modified aptamer displays the structure-switching signaling when it undergoes a structural change [16,17]. When the fluorophore-labeled aptamer binds to a small oligonucleotide labeled with a quencher to form a duplex structure, a large decrease in fluorescence intensity occurs. The target-induced signaling can be used as a probe for real-time kinetics of the binding reaction between the aptamer and target. Studies based on the application of signaling aptamers have been reported recently. Specifically, the enzymatic activity of the conversion of adenosine 5′-monophosphate (AMP) into adenosine by alkaline phosphate (ALP) has been monitored [18]. Another example is the development of a screening assay for adenosine deaminase (ADA) [19]. Moreover, the adsorption and covalent coupling of the DNA aptamer onto cellulose have been studied in order to develop a bioactive paper [20].

Since the signaling DNA aptamer serves as a real-time reporter, rate constants for the binding reaction can be derived from the fluorescence intensity in principle [21]. In our study, specifically designed experiments for the binding reaction of signaling DNA aptamer, QDNA (quencher), and adenosine 5′ triphosphate (ATP) target in solution have been performed. The reaction is observed by monitoring the fluorescence intensity. The experimental procedure is developed in Ref. [18] and briefly presented in Sec. II. In order to study the observed fluorescence intensities, we propose a kinetic model for the binding of signaling DNA aptamers to quenchers and ATP targets in Sec. III. The modeling allows us to deduce relevant reactions. The corresponding rate constants are determined by fitting the model prediction with the normalized fluorescence intensity. Although the bimolecular

*nakamur@physics.mcmaster.ca
†shi@mcmaster.ca
‡Present address: Department of Biology, Massachusetts Institute of Technology, Cambridge, MA 02139-4307, USA.

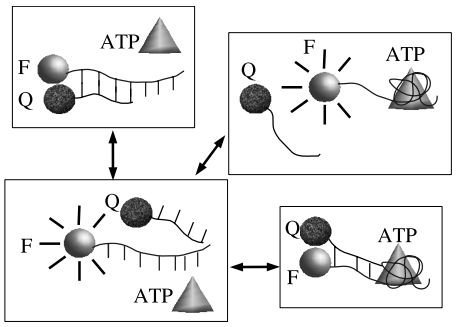

FIG. 1. The schematic description for the binding reaction of DNA aptamer, QDNA (quencher), and ATP target. When the DNA aptamer (F) and the quencher (Q) are dissociated, the fluorescence arises (lower left and upper right). The binding between the DNA aptamer and the quencher induces a large decrease in the fluorescence intensity (lower right and upper left). The lower right figure shows that the quencher binds to the DNA aptamer-ATP complex.

binding process to form DNA aptamer-ATP complex has been established experimentally [16], the kinetic modeling indicates that other possible side reactions exist for the structure-switching DNA aptamer. A proposed reaction is the simultaneous complexation of the three molecules. The schematics of the binding process are shown in Fig. 1. Furthermore, we show that the agreement between the theoretical model and the experiment can be improved with the possibility of a misfolded state of the DNA aptamer, as discussed in Sec. IV.

II. EXPERIMENTS

In our specifically designed experiments, DNA oligonucleotides labeled with a fluorophore at the 5′ end of the stem (FAM) and a quencher at 3′ end (Dabcyl) were used as DNA aptamer (FDNA) and antisense DNA (QDNA), as shown in Fig. 2. The FDNA/ATP complex is expected to show the structure-switching mechanism in the presence of QDNA because the binding of QDNA induces a large decrease in fluorescence intensity [16,18]. Since a longer QDNA provides more base sequences complementary to those of FDNA, they are capable of forming the duplex structure more tightly. Note that the DNA aptamer is longer than QDNAs. Therefore, the DNA duplex possesses a long dangling end whose base sequence is not complementary to the shorter QDNAs.

DNA Aptamer

5' – FAM - TCACTGACCTGGGGGAGTATTGCGGAGGAAGGT

Quenchers

Q10 3' - Dabcyl – GTGACTGGAC – 5'
Q11 3' - Dabcyl – GTGACTGGACC – 5'
Q12 3' - Dabcyl – GTGACTGGACCC – 5'
Q13 3' - Dabcyl – GTGACTGGACCCC – 5'

FIG. 2. ATP-binding DNA aptamer and antisence DNA as a model system. Q10, Q11, Q12, and Q13 denote, respectively, the number of base sequences. For example, Q10 has 10 base sequences.

In the experiments, the following concentrations of oligonucleotides were used for fluorescence measurements: 20 nM for FDNA, 40 nM for QDNA, and 0.75 mM for ATP. The assay buffer contained NaCl (300 mM), $MgCl_2$ (5 mM), and HEPES [4-(2-hydroxyethyl)-1-piperazineethanesulfonic acid] (25 mM, pH 8.0). Fluorescence intensities were recorded on a Cary Eclipse fluorescence spectrophotometer (Varian) with excitation at 490 nm and emission at 520 nm. The sample volume was 0.5 ml in all cases. For the FDNA(F)+QDNA(Q) reaction, a mixture of FDNA in assay buffer (494.25 μl) and water (3.75 μl) was incubated at 23 °C for 24 h. The theoretical melting temperatures of the QDNAs (Q10–Q13) were estimated at T_m=35 (Q10), 41 (Q11), 47 (Q12), and 52(Q13) °C by using UNAFold from the DINAMelt web server [22–24]. For the FDNA/ATP complex (FT)+QDNA reaction, a mixture of FDNA in assay buffer (494.25 μl) and ATP (3.75 μl) was also incubated at 23 °C for 24 h. Fluorescence measurements were taken for background readings. As expected, no quenching of fluorescence occurred with the formation of DNA aptamer and ATP target complex. QDNA (2 μl) was then added and fluorescence readings were recorded every 15 s until equilibrium was reached. A large decrease in fluorescence emission due to quenching was observed. In the figures presented in this paper, we defined the time when the quenching reaction starts as an initial time, i.e., t=0. The fluorescence intensity in the binding reaction was recorded as a function of time. Each measurement was repeated at least five times for a given length of QDNA to ensure the reproducibility of the data.

III. KINETIC MODELS

A. Modeling for $F+Q$

Before considering the case with the ATP targets, a simple model for the reaction of DNA aptamer (F) and QDNA (Q) is studied first. For this purpose, the experiment was performed as follows. (a) QDNA is added into the solution of the DNA aptamers. (b) The fluorescence intensity which arises from the fluorophore attached on the DNA aptamer is observed during the binding reaction, and hence the time development of the intensity is obtained experimentally. The experimental data is then compared with theoretical predictions, which allow us to determine the rate constants of the model.

The binding reaction of F and Q is described by

$$F + Q \underset{k_1}{\overset{k_2}{\rightleftarrows}} FQ, \tag{1}$$

where k_1 and k_2 are two rate constants. The duplex DNA molecule is defined as FQ. In terms of the concentrations, this reaction model leads to the following set of kinetic equations:

$$\frac{d[F]}{dt} = k_1[FQ] - k_2[F][Q], \tag{2}$$

$$\frac{d[Q]}{dt} = k_1[FQ] - k_2[F][Q], \tag{3}$$

$$\frac{d[FQ]}{dt} = -k_1[FQ] + k_2[F][Q], \tag{4}$$

where the bracket denotes the molar concentration in solution. It follows from these equations that

$$[F] = [F]_0 + [FQ]_0 - [FQ], \tag{5}$$

$$[Q] = [Q]_0 + [FQ]_0 - [FQ], \tag{6}$$

where the subscript "0" indicates the initial concentrations of the reactants with which the binding reaction starts. These two relations are due to mass conservation. Although these differential equations are coupled with each other, an analytical solution can be obtained [25]. Specifically, Eqs. (5) and (6) enable us to write

$$\frac{d[FQ]}{dt} = -k_1[FQ] + k_2([F]_0 + [FQ]_0 - [FQ])([Q]_0 + [FQ]_0 - [FQ]). \tag{7}$$

The analytical solution of Eq. (7) is given by

$$\frac{[FQ]}{[FQ]_0} = x_1 x_2 \left(\frac{1 - \exp(-k_{eff}t)}{x_2 - x_1 \exp(-k_{eff}t)} \right), \tag{8}$$

where the parameters are

$$x_1 = \frac{1 + (1+b)\alpha - \sqrt{(1+\alpha+b\alpha)^2 - 4b\alpha^2}}{2\alpha}, \tag{9}$$

$$x_2 = \frac{1 + (1+b)\alpha + \sqrt{(1+\alpha+b\alpha)^2 - 4b\alpha^2}}{2\alpha}, \tag{10}$$

$$b = \frac{[Q]_0}{[F]_0}, \tag{11}$$

$$\alpha = \frac{k_2[F]_0}{k_1}, \tag{12}$$

$$k_{eff} = \sqrt{(1+\alpha+b\alpha)^2 - 4b\alpha^2}\, k_1. \tag{13}$$

Here, α and k_{eff} determine, respectively, the long-time steady-state solution and the relaxation time of the differential equations. The fluorescence intensity, I, arising from the DNA aptamer is assumed to be proportional to the concentration of the DNA aptamer, i.e.,

$$I = (\text{const})[F]. \tag{14}$$

The initial fluorescence intensity, I_0, is obtained by the average value before QDNA is added into the solution of the DNA aptamer. The normalized fluorescence intensity, $\tilde{I} = I/I_0$, can be cast into the form,

$$\tilde{I} = \frac{[F]}{[F]_0} = 1 + \frac{[FQ]_0}{[F]_0} - \frac{[FQ]}{[F]_0}. \tag{15}$$

The optimization to determine the two parameters can be achieved by the least-squares fitting of the difference between the experiments and theory. The calculation, however, is simplified by using $\tilde{I}$ in equilibrium. At $t \to \infty$, Eqs. (8) and (15) lead to

$$\tilde{I}(t \to \infty) = 1 - \frac{1 + \alpha + b\alpha - \sqrt{(1+\alpha+b\alpha)^2 - 4b\alpha^2}}{2\alpha}. \tag{16}$$

In our experiment, we used $[F]_0 = 20$ nM, $[Q]_0 = 40$ nM, and $[FQ]_0 = 0$ nM at 23 °C. Thus, the parameter in the model, α, is determined by the experimental observation of $\tilde{I}$ in equilibrium. The other parameter, k_{eff}, can be obtained by the relaxation time of the experimental fluorescence intensity. This method of determining the parameters by using $\tilde{I}$ in equilibrium reduces the number of parameters in the model, which in turn reduces the cost of the numerical calculation, especially in the case that there are a number of reactants. We will use this strategy again in the following section for the binding reaction with ATP target.

B. Modeling for $FT+Q$

In this section, we assume that the bimolecular binding of a DNA aptamer and an ATP target does not induce a change in the fluorescence intensity since the conformational change is not associated with QDNA. Therefore, the addition of ATP targets itself does not provide information about the binding reaction. However, once QDNA is added into the solution, it will bind to a DNA aptamer, leading to a decrease in the fluorescence intensity or quenching. For these reactions, we propose the following kinetic model:

$$F + Q \underset{k_1}{\overset{k_2}{\rightleftarrows}} FQ, \tag{17}$$

$$F + T \underset{k_3}{\overset{k_4}{\rightleftarrows}} FT, \tag{18}$$

$$F + T + Q \underset{k_5}{\overset{k_6}{\rightleftarrows}} FTQ, \tag{19}$$

where T, FT, and FTQ denote, respectively, ATP target, DNA aptamer-ATP complex, and the complex which consists of a DNA aptamer, QDNA, and an ATP target. The parameters, $k_1 \sim k_6$, are the reaction rates. Here, it is assumed that the DNA aptamer-ATP complex is directly formed between an ATP target and a free-target binding site of the DNA aptamer, as well as between an ATP target and the DNA aptamer which is possibly occupied by QDNA [16]. Therefore, the complex is considered to be quenched by QDNA, whereas it maintains to bind an ATP target, and hence it cannot provide fluorescence. We have attempted to fit the experimental $\tilde{I}$ for different length of QDNAs first without such an additional complex state [Eq. (19)]. However, we were not able to obtain a consistent set of parameters which reproduce the experimental data [26]. The theoretical duplex structures of the DNA aptamer and Q10–Q13 were evaluated by using UNAFold. Nonpaired binding sites of the DNA aptamer do not lead to a hairpin loop at 23 °C as the most

stable structure. The free-target-binding sites of FQ for the ATP target are provided. We concluded that the simple bimolecular binding reaction does not provide a complete description of the experimental data, especially during the binding reaction. Consequently, side reactions such as the complex formation [Eq. (19)] are required in order to explain the intermediate state in the reactions.

The kinetic equations derived from our model [Eqs. (17)–(19)] are

$$\frac{d[F]}{dt} = k_1[FQ] - k_2[F][Q] + k_3[FT] - k_4[F][T] + k_5[FTQ] - k_6[F][T][Q], \tag{20}$$

$$\frac{d[Q]}{dt} = k_1[FQ] - k_2[F][Q] + k_5[FTQ] - k_6[F][T][Q], \tag{21}$$

$$\frac{d[FQ]}{dt} = -k_1[FQ] + k_2[F][Q], \tag{22}$$

$$\frac{d[T]}{dt} = k_3[FT] - k_4[F][T] + k_5[FTQ] - k_6[F][T][Q], \tag{23}$$

$$\frac{d[FT]}{dt} = -k_3[FT] + k_4[F][T], \tag{24}$$

$$\frac{d[FTQ]}{dt} = -k_5[FTQ] + k_6[F][T][Q]. \tag{25}$$

There are six parameters to be determined in these coupled differential equations. These parameters are optimized such that they provide a best fit to the experimental fluorescence intensity for different length of QDNAs. One can derive the conservation of the mass from the equations,

$$[FTQ] + [FT] + [T] = [FTQ]_0 + [FT]_0 + [T]_0, \tag{26}$$

$$[FTQ] + [FQ] + [Q] = [FTQ]_0 + [FQ]_0 + [Q]_0, \tag{27}$$

$$[FTQ] + [FQ] + [F] + [FT] = [FTQ]_0 + [FQ]_0 + [F]_0 + [FT]_0. \tag{28}$$

These relations allow us to reduce the number of independent differential equations to three,

$$\frac{d[FT]}{dt} = -k_3[FT] + k_4([FTQ]_0 + [FQ]_0 + [F]_0 + [FT]_0 - [FT] - [FQ] - [FTQ])([FTQ]_0 + [FT]_0 + [T]_0 - [FT] - [FTQ]), \tag{29}$$

$$\frac{d[FQ]}{dt} = -k_1[FQ] + k_2([FTQ]_0 + [FQ]_0 + [F]_0 + [FT]_0 - [FT] - [FQ] - [FTQ])([FTQ]_0 + [FQ]_0 + [Q]_0 - [FQ] - [FTQ]), \tag{30}$$

$$\frac{d[FTQ]}{dt} = -k_5[FTQ] + k_6([FTQ]_0 + [FQ]_0 + [F]_0 + [FT]_0 - [FT] - [FQ] - [FTQ])([FTQ]_0 + [FT]_0 + [T]_0 - [FT] - [FTQ])([FTQ]_0 + [FQ]_0 + [Q]_0 - [FQ] - [FTQ]). \tag{31}$$

In our experiment, the initial concentrations at 23 °C are

$$[F]_0 = 20 \text{ nM}, \quad [Q]_0 = 40 \text{ nM}, \quad [T]_0 = 0.75 \text{ mM}, \quad [FQ]_0 = 0 \text{ nM}, \quad [FT]_0 = 0 \text{ nM}, \quad \text{and } [FTQ]_0 = 0 \text{ nM}. \tag{32}$$

By using these conditions, one obtains the following nondimensional coupled differential equations,

$$\gamma\frac{dx}{d\tau} = -x + \beta(1 - x - y - z)(b - x - z), \tag{33}$$

$$\frac{dy}{d\tau} = -y + \alpha(1 - x - y - z)(c - y - z), \tag{34}$$

$$\frac{dz}{d\tau} = -\xi z + \eta(1 - x - y - z)(b - x - z)(c - y - z), \tag{35}$$

where the normalized conditions are x, y, z, and b, c, τ, α, β, γ, η, and ξ are parameters,

$$x = \frac{[FT]}{[F]_0}, \quad y = \frac{[FQ]}{[F]_0}, \quad z = \frac{[FTQ]}{[F]_0},$$

$$b = \frac{[T]_0}{[F]_0} = 37\,500, \quad c = \frac{[Q]_0}{[F]_0} = 2,$$

$$\tau = k_1 t, \quad \alpha = \frac{k_2[F]_0}{k_1}, \quad \beta = \frac{k_4[F]_0}{k_3},$$

$$\gamma = \frac{k_1}{k_3}, \quad \eta = \frac{k_6[F]_0^2}{k_1}, \quad \text{and} \quad \xi = \frac{k_5}{k_1}. \tag{36}$$

As discussed in the modeling for $F + Q \leftrightarrow FQ$, k_1 and k_2 can be determined independently from the $F + Q$ experiments. Thus, α is considered to be a given parameter. The normalized fluorescence intensity in this case becomes

$$\tilde{I} = \frac{[F] + [FT]}{[F]_{\text{ini}} + [FT]_{\text{ini}}}. \tag{37}$$

The bracket with "ini" denotes the concentration at the time when QDNA is added into the solution where the binding reaction, $F + T \leftrightarrow FT$, is in equilibrium. Therefore, before

quenching is initiated, the reaction between the DNA aptamer and an ATP target is simply described as a bimolecular reaction, whose forms of the rate law are similar to Eqs. (2)–(4). Since those equations obey the conservation of the mass,

$$[F]_{\mathrm{ini}} + [FT]_{\mathrm{ini}} = [F]_0 + [FT]_0. \tag{38}$$

Equations (28) and (38) lead to

$$\tilde{I} = 1 - y - z. \tag{39}$$

This allows us to obtain $\tilde{I}$ from y and z by solving Eqs. (33)–(35), which can be compared to the observed fluorescence intensities.

C. Constraints on the parameters

In order to reduce the number of independent parameters to be determined in the model, the following constraints on β are derived. By setting $\frac{dx}{d\tau}=0$, $\frac{dy}{d\tau}=0$, and $\frac{dz}{d\tau}=0$, one can show that the steady-state solutions satisfy

$$x_{\mathrm{eq}} = \beta(1 - x_{\mathrm{eq}} - y_{\mathrm{eq}} - z_{\mathrm{eq}})(b - x_{\mathrm{eq}} - z_{\mathrm{eq}}), \tag{40}$$

$$y_{\mathrm{eq}} = \alpha(1 - x_{\mathrm{eq}} - y_{\mathrm{eq}} - z_{\mathrm{eq}})(c - y_{\mathrm{eq}} - z_{\mathrm{eq}}), \tag{41}$$

$$\xi z_{\mathrm{eq}} = \eta(1 - x_{\mathrm{eq}} - y_{\mathrm{eq}} - z_{\mathrm{eq}})(b - x_{\mathrm{eq}} - z_{\mathrm{eq}})(c - y_{\mathrm{eq}} - z_{\mathrm{eq}}), \tag{42}$$

where the subscript "eq" denotes the value in equilibrium.

Therefore, it follows from $\tilde{I}_{\mathrm{eq}}=1-y_{\mathrm{eq}}-z_{\mathrm{eq}}$ that

$$x_{\mathrm{eq}} = \beta(\tilde{I}_{\mathrm{eq}} - x_{\mathrm{eq}})(b - x_{\mathrm{eq}} - z_{\mathrm{eq}}), \tag{43}$$

$$y_{\mathrm{eq}} = \alpha(\tilde{I}_{\mathrm{eq}} - x_{\mathrm{eq}})(c - 1 + \tilde{I}_{\mathrm{eq}}), \tag{44}$$

$$\xi z_{\mathrm{eq}} = \eta(\tilde{I}_{\mathrm{eq}} - x_{\mathrm{eq}})(b - x_{\mathrm{eq}} - z_{\mathrm{eq}})(c - 1 + \tilde{I}_{\mathrm{eq}}). \tag{45}$$

It is easy to show that these nonlinear equations lead to

$$0 = \frac{\beta y_{\mathrm{eq}}}{\alpha(c - 1 + \tilde{I}_{\mathrm{eq}})}\left[b + y_{\mathrm{eq}} - 1 + \frac{y_{\mathrm{eq}}}{\alpha(c - 1 + \tilde{I}_{\mathrm{eq}})}\right] + \frac{y_{\mathrm{eq}}}{\alpha(c - 1 + \tilde{I}_{\mathrm{eq}})} - \tilde{I}_{\mathrm{eq}}, \tag{46}$$

where

$$y_{\mathrm{eq}} = \frac{\eta\tilde{I}_{\mathrm{eq}}(c - 1 + \tilde{I}_{\mathrm{eq}}) - \beta\xi(1 - \tilde{I}_{\mathrm{eq}})}{\left(\frac{\eta}{\alpha} - \beta\xi\right)}. \tag{47}$$

This equation indicates that once the normalized fluorescence intensity at equilibrium is measured experimentally, β can be obtained as a function of η and ξ. By using this constraint, we determine the other parameters, γ, η, and ξ, numerically so that our theoretical results fit the experimental $\tilde{I}$ for different length of QDNAs. Furthermore, the fact that k_3 and k_4 are not directly related to the reaction for QDNA leads us to the consideration that they should not vary among the experiments for different length of QDNAs. This provides us with another constraint for these two parameters, η and ξ. With these constraints taken, our six parameters can be obtained more accurately by minimizing the least-squares difference. The fitting requires the numerical calculation to solve the coupled ordinary differential equations for the rate law. Here, let us summarize the procedure of the analysis to clarify the method to fit the rate constants. First, we determine k_1 and k_2 by the two-state model [Eq. (1)]. This experiment is independently performed before the one with ATP targets. Thus, one can fix α. Second, when the experimental $\tilde{I}_{\mathrm{eq}}$ is obtained, it follows from Eqs. (46) and (47) that $\beta=\beta(\eta,\xi)$. Third, the theoretical $\tilde{I}$ as a function of t, which is derived from Eqs. (33)–(35) and (39) with γ, η and ξ, is fit to reproduce the experimental $\tilde{I}$ with the constraint that k_3 and k_4 are not altered for different values of α.

TABLE I. The parameters determined by the five-repeated experiments for different length of QDNAs.

	k_1 (1/s)	k_2 (1/s M)	α
Q10	0.420 ± 0.025	$0.470\times10^8 \pm 0.064\times10^8$	2.2 ± 0.2
Q11	0.095 ± 0.009	$0.383\times10^8 \pm 0.051\times10^8$	8.1 ± 0.3
Q12	0.029 ± 0.005	$0.176\times10^8 \pm 0.050\times10^8$	12.3 ± 1.0
Q13	0.028 ± 0.003	$0.304\times10^8 \pm 0.064\times10^8$	21.6 ± 2.4

IV. RESULTS AND DISCUSSION

Optimized parameters for the $F+Q$ reaction are given in Table I. For a given length of QDNA, the experiment was repeated five times. As seen in the table, the dissociation rate of the DNA duplex, k_1, decreases as QDNA becomes longer. This is reasonable because longer QDNA has more base pairs with hydrogen bondings, which should tend to bind the DNA aptamer more tightly once the duplex DNA is formed. Based on energetic consideration, we expect that $k_1 \sim e^{-G_d/k_BT}$, where G_d is the binding free energy of the DNA aptamer and QDNA. In Fig. 3, $\ln k_1$ is plotted as a function

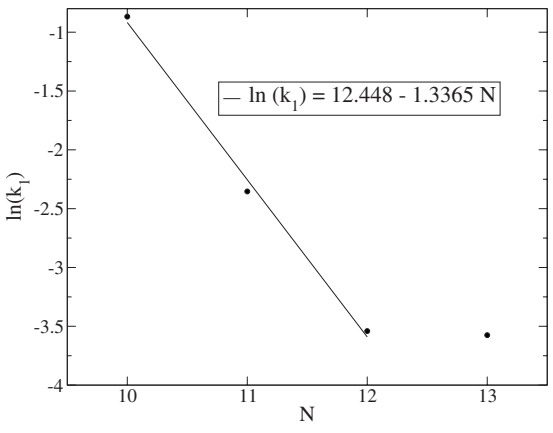

FIG. 3. The dissociation rate of FQ, k_1, as a function of N. The line denotes the linear regression of three points for Q10, Q11, and Q12.

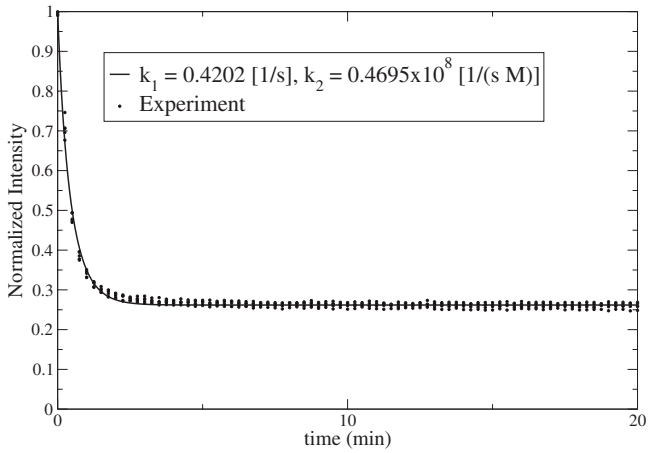

FIG. 4. Normalized fluorescence intensity for Q10 in the reaction of $F+Q$ at 23 °C. The dotted lines and solid line correspond to the five-repeated experiments and theoretical result, respectively.

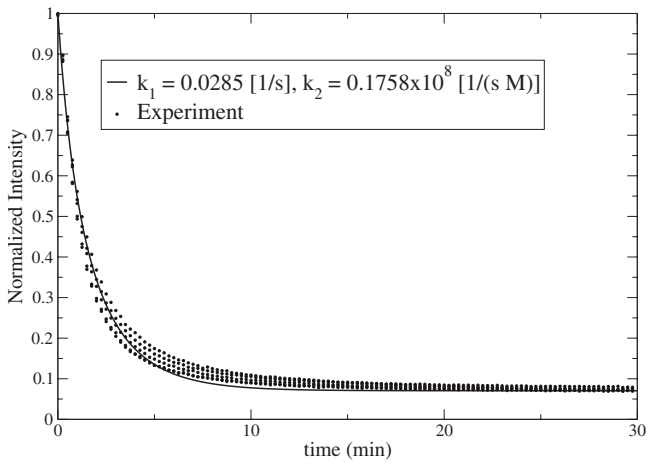

FIG. 6. Normalized fluorescence intensity for Q12 in the reaction of $F+Q$ at 23 °C. The dotted lines and solid line correspond to the five-repeated experiments and theoretical result, respectively.

of the number of base pairs, N. A linear relation between G_d and N is obtained for Q10, Q11, and Q12. The binding free energy per base pair is estimated at $-1.3k_BT$. This is in good agreement with the results of unzipping of DNA double helix by Cocco *et al.* [27] and opening rates of molecular beacons by Fradin [28]. These studies indicated $G_d=-1.4k_BT-$ $-1.6k_BT$. The weaker dependence of k_1 with Q13 implies that the last sequences of the DNA aptamer and QDNA may not provide a complete binding, leading to a dangling end. In addition, the association rate of the DNA duplex, k_2, varies only within the same order of magnitude. The association rate of the DNA duplex is largely determined by the collision of binding sites of the DNA aptamer and QDNA [29]. Therefore, the relatively small change in duplex length does not lead to a large variation in k_2. As defined in Eq. (12), α is proportional to the association constant, which is expected to increase for a longer QDNA. Our results confirm such a behavior as shown in Table I. Figures 4–7 show the normalized fluorescence intensities for different length of QDNAs with the optimized parameters. It is clearly seen that the calculations based on the two-state model provide very good descriptions of the experimental observations. However, small deviations for the relaxation of the reaction are visible as QDNA becomes longer. Since some base pairs on the DNA aptamer are complementary to not only base pairs on QDNA but also base pairs on the DNA aptamer itself, the single-stranded DNA misfolds itself to form secondary structures [30]. Many possible misfolded structures at 23 °C are obtained with the sequence of the DNA aptamer by using UNAFold. The discrepancy of the normalized fluorescence intensities can be substantially eliminated without changing the rate constants for Eq. (1) when we include a further reaction in the model,

$$F \underset{k_u}{\overset{k_f}{\rightleftarrows}} F^*, \tag{48}$$

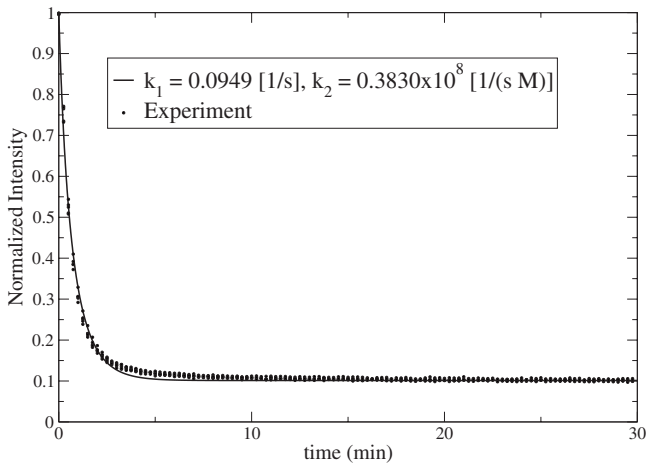

FIG. 5. Normalized fluorescence intensity for Q11 in the reaction of $F+Q$ at 23 °C. The dotted lines and solid line correspond to the five-repeated experiments and theoretical result, respectively.

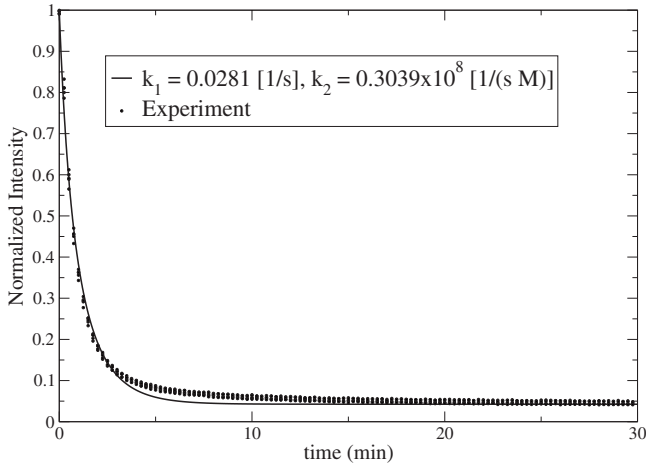

FIG. 7. Normalized fluorescence intensity for Q13 in the reaction of $F+Q$ at 23 °C. The dotted lines and solid line correspond to the five-repeated experiments and theoretical result, respectively.

TABLE II. The rate constants which provide an agreement with the experimental fluorescence intensity for different length of QDNAs.

	k_3 (1/s)	k_4 (1/s M)	k_5 (1/s)	k_6 (1/s M^2)	K_d (μM)
Q10	0.854 ± 0.273	$0.165 \times 10^7 \pm 0.142 \times 10^7$	303 ± 251	$0.507 \times 10^{15} \pm 0.473 \times 10^{15}$	1.4 ± 1.1
Q11	0.854 ± 0.273	$0.165 \times 10^7 \pm 0.142 \times 10^7$	45.7 ± 42.6	$0.568 \times 10^{15} \pm 0.522 \times 10^{15}$	1.4 ± 1.1
Q12	0.854 ± 0.273	$0.165 \times 10^7 \pm 0.142 \times 10^7$	8.98 ± 5.89	$0.181 \times 10^{15} \pm 0.134 \times 10^{15}$	1.4 ± 1.1
Q13	0.854 ± 0.273	$0.165 \times 10^7 \pm 0.142 \times 10^7$	1.50 ± 1.41	$0.185 \times 10^{15} \pm 0.166 \times 10^{15}$	1.4 ± 1.1

where F^* denotes the misfolded state of the DNA aptamer which blocks the binding of QDNA. The least-squares fitting for Eqs. (1) and (48) leads to $k_f = 0.001 - 0.004$ (1/s), $k_u = 0.03 - 0.095$ (1/s), and $k_f/k_u = 0.017 - 0.04$ for Q10, Q11, Q12, and Q13. The ratio of k_f and k_u indicates that the misfolded DNA aptamers in equilibrium are about a few percentage of free single-stranded DNA aptamers. The variation in the two parameters is small since they should be independent of the presence of QDNA. The free-energy difference, dG^*, between F and F^* is estimated at 1.9–2.4 kcal/mol, assuming $k_f/k_u = e^{(-dG^*/k_BT)}$. There are about ten misfolded states with dG^* falling in this range, and hence it is plausible to assume that QDNA cannot bind to some of these misfolded DNA aptamers at 23 °C. For example, T_m of the free binding sites of one misfolded DNA aptamer and QDNA is estimated at 14 °C. Thus, the results imply that one (or some) of the misfolded states blocks the binding of QDNA during the reaction.

The rate constants, k_1 and k_2, determined from the $F+Q$ reactions, are employed to fit the normalized fluorescence intensity for the reaction with ATP targets. Table II gives the numerically determined rate constants and the dissociation constant for $FT+Q$. The data fitting leads to a relatively large variation in the rate constants, k_4, k_5, and k_6, implying that more side reactions may exist in the kinetics of the complexation. We have not attempted to narrow the ranges of the parameters mainly because of the limited information from the experiments. As shown in Fig. 8, the theoretical $\tilde{I}$ with the parameters for Q13 displays a good agreement with the experimental observation. Similarly, we found that the theoretical results for Q10, Q11, and Q12 provide equally good descriptions of the experimental data. As a further test of the model, a set of parameters for Q10 determined here provides a good description for experiments with different initial concentrations, $[F]_0 = 60$ nM, $[Q]_0 = 30$ nM, and $[T]_0 = 0.9$ mM (Fig. 8). Note that as the length of QDNA becomes longer, the dissociation rate of FTQ, k_5, tends to become smaller with respect to increase the number of binding sites on QDNA. This is similar to the case of the simple binding reaction for $F+Q \leftrightarrow FQ$. As discussed before, the same reason for the small variation in k_2 explains the fact that k_6 also does not show a large change with respect to length of QDNA. The concentration of each reactant with a set of parameters for Q13 is shown in Fig. 9. QDNA prefers to form FTQ rather than the simple DNA aptamer-QDNA duplex (FQ) since in our experimental condition abundant ATP molecules exist in solution while QDNA interacts with the DNA aptamer, forming the complex.

The determination of the rate constants provides an estimate of the dissociation constant,

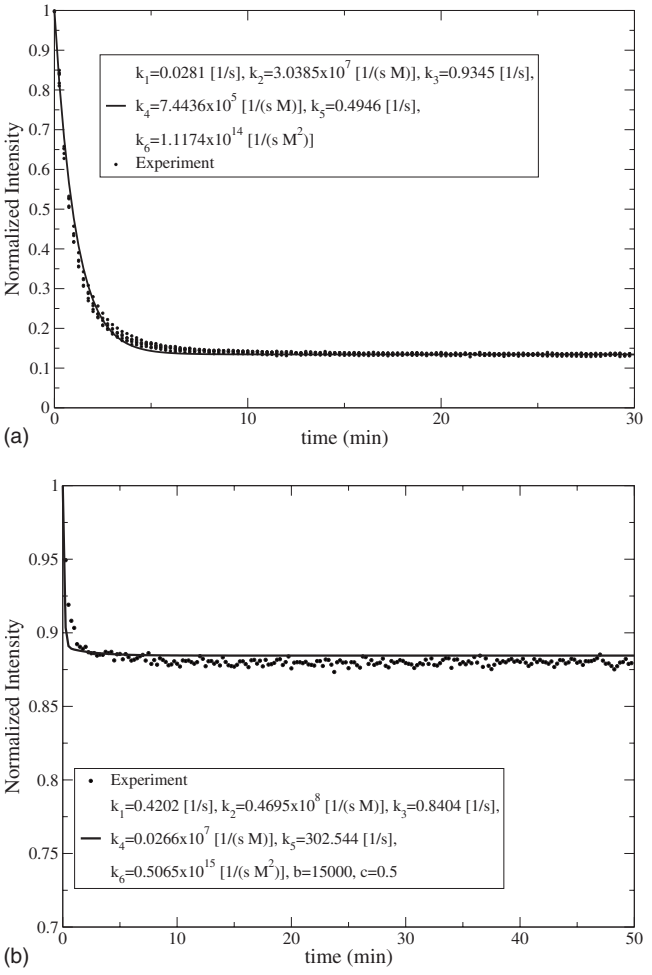

FIG. 8. Comparison of the experimental normalized fluorescence intensities for Q13 and Q10 at 23 °C to the calculated results. The theoretical result with a solid line is obtained by a set of parameters determined by minimizing the least-squares difference. The five dotted lines for Q13 denote, respectively, the five-repeated experiments in the same condition that QDNA is added to the solution of the DNA aptamer and ATP target. The parameters for Q10 at 23 °C which we determined in the condition, $[F]_0 = 20$ nM, $[Q]_0 = 40$ nM, and $[T]_0 = 0.75$ mM, were employed to calculate the normalized fluorescence intensity for Q10 at 23 °C with the different concentration, $[F]_0 = 60$ nM, $[Q]_0 = 30$ nM, and $[T]_0 = 0.9$ mM.

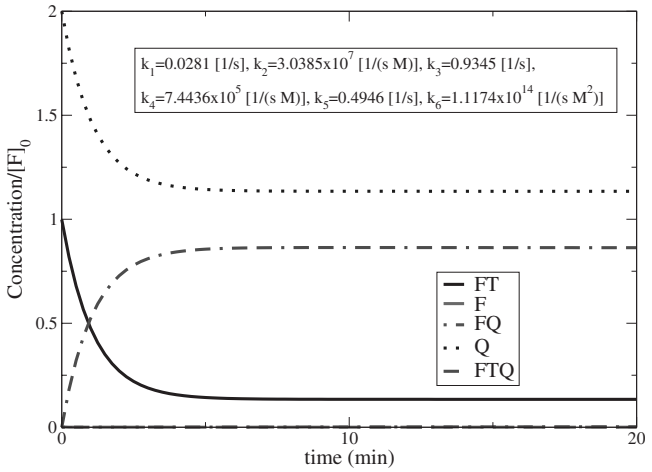

FIG. 9. Time development for the concentration of each reactant scaled by $[F]_0$. The calculation was performed with $[F]_0=20$ nM, $[Q]_0=40$ nM, and $[T]_0=0.75$ mM. The concentration of the ATP target is not shown in the figure. As seen in the figure, the production of (F) and (FQ) are relatively small during the reaction.

$$K_d = \frac{[F]_{\mathrm{eq}}[T]_{\mathrm{eq}}}{[FT]_{\mathrm{eq}}} = 0.3 - 2.5 \ \mu\mathrm{M}. \tag{49}$$

This is a typically expected value of DNA aptamers designed for the target of small molecules [16,31]. Thus, the kinetic modeling gives us a simple method to obtain the kinetic parameters without performing laborious experiments. The determined values can be used for different operating conditions or further development of the model with different species mixtures.

In summary, specifically designed experiments for the binding reaction of signaling DNA aptamer, QDNA, and ATP target in solution have been performed. A kinetic model of the DNA aptamer binding has been developed. It has been demonstrated that the theoretical model provides a good description of the experiments. Rate constants are determined by comparing the model predictions with the experiments. We found that the bimolecular model described by Eqs. (17) and (18) did not sufficiently reproduce the experimental fluorescence intensities. Therefore, the three-body binding reaction [Eq. (19)] was proposed in our kinetic model. The addition of the side reaction provided good agreements between the theory and experiments. As shown in Tables I and II, the resultant rate constants for the dissociation of QDNA vary in accordance with the number of binding sites. Furthermore, small discrepancies of $\tilde{I}$ between the theory and experiments for the reaction of DNA aptamer and QDNA are removed when the misfolded state of the DNA aptamer [Eq. (48)] is included. The misfolded structure blocks the binding of QDNA. This reduces quenching of the fluorescence intensity during the reaction. Hence, the kinetic modeling of DNA aptamer, QDNA, and ATP target allows us to obtain the relevant kinetic process in the binding reaction. The kinetic study can also be applied to other nucleic acid aptamers to extract information about the structural property in the reaction. This will be expected to support in studying the functioning in biological systems or the development of bioanalytical molecular tools.

ACKNOWLEDGMENTS

This work was supported by the Natural Science and Engineering Research Council of Canada (NSERC). We would like to thank Dr. Cecile Fradin for many useful discussions on DNA binding.

[1] R. R. Breaker, Nature (London) **432**, 838 (2004).
[2] M. Fried and D. M. Crothers, Nucleic Acids Res. **9**, 6505 (1981).
[3] M. M. Garner and A. Revzin, Nucleic Acids Res. **9**, 3047 (1981).
[4] L. F. Melo, S. T. Mundle, M. H. Fattal, N. E. O'Regan, and P. R. Strauss, DNA Repair (Amst.) **6**, 374 (2007).
[5] G. A. Soukup and R. R. Breaker, RNA **5**, 1308 (1999).
[6] A. Nahvi, N. Sudarsan, M. S. Ebert, X. Zou, K. L. Brown, and R. R. Breaker, Chem. Biol. **9**, 1043 (2002).
[7] K. Aslan, J. R. Lakowicz, and C. D. Geddes, Curr. Opin. Chem. Biol. **9**, 538 (2005).
[8] M. H. Hou, S. B. Lin, J. M. P. Yuann, W. C. Lin, A. H. J. Wang, and L. S. Kan, Nucleic Acids Res. **29**, 5121 (2001).
[9] Y. Gao, L. K. Wolf, and R. M. Georgiadis, Nucleic Acids Res. **34**, 3370 (2006).
[10] S. Jhaveri, M. Rajendran, and A. D. Ellington, Nat. Biotechnol. **18**, 1293 (2000).
[11] S. Jhaveri, R. Kirby, R. Conrad, E. Maglott, M. Bowser, R. T. Kennedy, G. Glick, and A. D. Ellington, J. Am. Chem. Soc. **122**, 2469 (2000b).
[12] J. R. Lakowicz, *Principles of Fluorescence Spectroscopy* (Plenum, New York, 1999), pp. 1–23.
[13] M. I. Wallace, L. M. Ying, S. Balasubramanian, and D. Klenerman, J. Phys. Chem. B **104**, 11551 (2000).
[14] G. Altan-Bonnet, A. Libchaber, and O. Krichevsky, Phys. Rev. Lett. **90**, 138101 (2003).
[15] S. A. E. Marras, F. R. Kramer, and S. Tyagi, Nucleic Acids Res. **30**, e122 (2002).
[16] R. Nutiu and Y. Li, J. Am. Chem. Soc. **125**, 4771 (2003).
[17] R. Nutiu and Y. Li, Angew. Chem., Int. Ed. **44**, 1061 (2005).
[18] R. Nutiu, J. M. Y. Yu, and Y. Li, ChemBioChem **5**, 1139 (2004).
[19] N. H. Elowe, R. Nutiu, A. Allah-Hassani, J. D. Cechetto, D. W. Hughes, Y. Li, and E. D. Brown, Angew. Chem., Int. Ed. **45**, 5648 (2006).
[20] S. Su, R. Nutiu, C. D. M. Filipe, Y. Li, and R. Pelton, Langmuir **23**, 1300 (2007).
[21] A. Reuter, W. U. Dittmer, and F. C. Simmel, Eur. Phys. J. E **22**, 33 (2007).
[22] N. R. Markham and M. Zuker, Nucleic Acids Res. **33**, W577 (2005).

[23] M. Zuker, Nucleic Acids Res. **31**, 3406 (2003).
[24] http://www.bioinfo.rpi.edu/applications/mfold/; http://dinamelt.bioinfo.rpi.edu/
[25] J. I. Steinfeld, J. S. Francisco, and W. L. Hase, *Chemical Kinetics And Dynamics* (Prentice-Hall, Englewood Cliffs, NJ, 1989).
[26] When only bimolecular reactions [Eqs. (17) and (18)] were used in order to obtain good fitting to the experiments we needed to put $k_3=0.02-0.04\times10^{-3}$, 42.7–0.04, 195–0.06, and 0.51–0.14(1/s) for Q10, Q11, Q12, and Q13, respectively. However, as discussed in Sec. IV, k_3 should not vary with the length of QDNA because it is not directly related to the reactions between the DNA aptamer and QDNA. Thus, we concluded that bimolecular reactions alone do not provide a consistent description of the experiments.
[27] S. Cocco, R. Monasson, and J. F. Marko, Proc. Natl. Acad. Sci. U.S.A. **98**, 8608 (2001).
[28] C. Fradin, private communication.
[29] G. Bonnet, O. Krichevsky, and A. Libchaber, Proc. Natl. Acad. Sci. U.S.A. **95**, 8602 (1998).
[30] A. Ansari, Y. Shen, and S. V. Kuznetsov, Phys. Rev. Lett. **88**, 069801 (2002).
[31] D. E. Huizenga and J. W. Szostak, Biochemistry **34**, 656 (1995).